Mechanics of Materials 16 (1993) 317–331
Elsevier

Bounds on the complex bulk modulus of a two-phase viscoelastic composite with arbitrary volume fractions of the components

L.V. Gibiansky [1] and R. Lakes [2]

WISCONSIN

The University of [redacted], *USA*

Received 23 October 1992; revised manuscript received 15 March 1993

The complex bulk modulus of an isotropic two phase composite material is analyzed in terms of the complex moduli of its phases. Bounds are developed for the complex bulk modulus $\kappa_* = \kappa'_* + i\kappa''_*$ of the composite with *arbitrary* volume fractions of phases. These bounds enclose a region in the complex plane (κ'_*, κ''_*) or in a stiffness loss map $(|\kappa_*|, \kappa''_*/\kappa'_* = \tan\delta)$. The frequency range is assumed to be well below frequencies associated with the inertial terms; the acoustic wavelength is much larger than the inhomogeneities. The bounds are obtained from the bulk modulus bounds by Gibiansky and Milton (1993, *Proc. R. Soc. London A440*, 163–188) for the two phase composites with *fixed* volume fractions of phases. The composite bulk modulus is shown to be constrained to a lens shaped region of the complex (κ'_*, κ''_*) plane by the outermost pair of several circular arcs, which depend on the component material properties. The bounds are investigated numerically to explore conditions which give rise to high loss combined with high stiffness. Composite microstructures corresponding to various points on the circular arcs are identified.

1. Introduction

Viscoelastic materials are used in the damping of mechanical vibration and in the absorption of sound. The loss tangent $\tan\delta$, or tangent of the phase angle δ between stress and strain in sinusoidal loading, is a useful measure of material damping. Common structural materials such as steel and aluminum, however, have small loss tangents. Conversely, the materials with high loss tangents tend to be compliant, hence not of structural interest. The future development of structural materials with a combination of stiffness and loss is expected to be aided by understanding of the bounds on the behaviour of viscoelastic composite materials.

Such bounds allow to predict the range of the properties of new composite materials without making costly experiments, they show the limits of improving the composite properties by changing the composition and the microstructure. The structures that achieve the bounds are important for optimal design problems.

There exists an extensive literature dealing with the bounds for the elastic composites (see Hashin and Shtrikman (1963), Avellaneda (1987), Cherkaev and Gibiansky (1993a) and references therein). Similar problems for the viscoelastic composites are more difficult to solve and the bounds that have been obtained were rather wide (see Hashin (1965, 1970), Christensen (1969), Roscoe (1969, 1972) and references therein) until the new variational principle for the description of the material with complex moduli has been suggested by Cherkaev and Gibiansky (1993b) (see also Milton (1990)). It was implemented by Gibiansky and Milton (1993) for bounding

Correspondence to: L.V. Gibiansky, Courant Institute of Mathematical Sciences, 251 Mercer Street, New York, NY 10012, USA.

[1] Supported by ONR, by Sloan Soviet Visitors Program and by Packard foundation through a fellowship of G.W. Milton.

[2] Supported by ONR and University of Iowa Faculty Scholars Program.

of the viscoelastic bulk modulus of the two-phase composites with *prescribed* proportions of phases. We use these results to bound the bulk modulus of a composite with *arbitrary* proportions of phases. Bounds on the complex bulk modulus of a material allow to estimate the dissipation in the composite under the action of the hydrostatic strain or stress fields.

It is well known (see, for example, Hashin (1970) and Christensen (1971)) that the behaviour of the viscoelastic materials at sufficiently low frequencies of oscillation can be described by the equations that formally coincide with the usual equations of elasticity but with complex strain and stress fields and complex moduli. The properties of the elastic isotropic material can be described by a pair of moduli. In engineering literature the Young's modulus E and the Poisson's ratio ν are used to characterize the properties of the material, in mathematical literature the bulk κ and shear μ moduli are used to describe the properties of an isotropic body. Both descriptions are equivalent and the relations between these pairs of moduli are given by the formulas

$$E = \frac{9\kappa\mu}{3\kappa + \mu}, \qquad \nu = \frac{3\kappa - 2\mu}{2(3\kappa + \mu)}, \tag{1.1}$$

or

$$\kappa = \frac{E}{3(1-2\nu)}, \qquad \mu = \frac{E}{2(1+\nu)}, \tag{1.2}$$

(see Christensen (1979), for example). Note also the helpful formula

$$\mu = c\kappa, \quad c = \frac{3(1-2\nu)}{2(1+\nu)}. \tag{1.3}$$

For the viscoelastic material all these moduli may have complex values and depend on the frequency of oscillations. We assume that the frequency is fixed and therefore the properties of the original materials are fixed as well.

In this paper we study the properties of the isotropic composite prepared from two isotropic viscoelastic materials. We are interested to find the range of the moduli which can be achieved by varying the volume fractions of the components and the geometry of the composite, i.e., the disposition of the phases in the composite. Such problem is known as a G_f-closure problem if the proportions of the components in the composite are fixed, or as a G-closure problem if these proportions are arbitrary (see, for example, Lurie and Cherkaev (1986), Kohn and Milton (1988), Cherkaev and Gibiansky (1992) and references therein). As we already mentioned, the properties of the isotropic viscoelastic material are characterized by two complex numbers (for example, by the bulk κ and shear μ moduli). To describe the set of the properties of all isotropic composites means to describe such set of pairs (κ_*, μ_*) that each point of this set corresponds to some composite and vice versa, the pair of the moduli (κ_*, μ_*) of any composite lies inside this set. It is a very difficult problem; a similar problem has not been solved even for the purely elastic composite when the properties of the isotropic material are described by only two parameters (real elastic moduli).

Here we restrict our attention only to the bounds for the complex bulk modulus. From this point of view each composite is characterized by only one complex number, namely by its bulk modulus κ. In the complex bulk modulus plane each composite corresponds to a point. If we fix the volume fraction f of the first phase and vary the structure of the composite over all possible microgeometries, this point traverses the region that we call $G_f(\kappa)$ set. If in addition we vary volume fraction f this set $G_f(\kappa)$ covers the region that we call $G(\kappa)$ set

$$G(\kappa) = \cup_{f\in[0,1]} G_f(\kappa). \tag{1.4}$$

We are interested to find the estimates on this $G(\kappa)$ set. Namely, we look for the bounds that provide the limit on the maximal extent of this region. They define the set $\widehat{G}(\kappa)$ that contains $G(\kappa)$, i.e., such that $G(\kappa) \subset \widehat{G}(\kappa)$. We also study the attainability of these bounds, i.e., look for the particular composites that possess the extremal bulk modulus.

The question of the minimal extent of similar to $G(\kappa)$ region has been explored by Chen and Lakes (1993) in the complex Young's modulus plane. They have plotted trajectories in the complex plane of Young's moduli associated with particular composite geometries including those which are extremal in the context of elastic modulus versus volume fraction. We show that some of those microgeometries also are extremal in the context of viscoelastic (i.e., complex) bulk modulus bounds.

In the paper by Gibiansky and Milton (1993) the bounds for the $G_f(\kappa)$ set, i.e., the set of the complex bulk moduli of the isotropic viscoelastic two-phase composites with *fixed* volume fractions of the phases were obtained and some microstructures which possess the extremal viscoelastic properties were found. We utilize these results in the present work to find the bound on the complex bulk modulus of the composite with *arbitrary* volume fractions of the phases and to find the microstructures that achieve these bounds.

Although we found the structures of the composites that correspond to some boundary points of the set $\widehat{G}(\kappa)$ (and therefore lie on the boundary of the $G(\kappa)$ set as well) it is not clear whether the set $G(\kappa)$ of all possible bulk moduli of two-phase composites coincides with the set $\widehat{G}(\kappa)$ that we found.

Throughout the paper we use the notations a' and a'' for the real and imaginary parts of the complex variable $a = a' + \mathrm{i}a''$, $\mathrm{i} = \sqrt{-1}$, the star in $a^* = a' - \mathrm{i}a''$ denotes the complex conjugate to a, and $|a| = \sqrt{(a')^2 + (a'')^2} = \sqrt{aa^*}$, $\arg(a) = \arctan(a''/a')$ denotes the absolute value and the argument of $a = |a|\exp(\mathrm{i}\arg(a))$. Symbols $\kappa_1, \mu_1, \kappa_2, \mu_2$ and κ_*, μ_* denote the complex bulk and shear moduli of the first and the second phases and the composite, respectively, and $\mathrm{Arc}(\alpha_1, \alpha_2, \alpha_3)$ denotes the arc of a circle in the complex plane joining the points α_1 and α_2 that when extended passes through α_3. One can check that such an arc is drawn by the point $\alpha(\gamma)$

$$\begin{aligned}\alpha(\gamma) &= \alpha_1 + \frac{1-\gamma}{1/(\alpha_2-\alpha_1) + \gamma/(\alpha_1-\alpha_3)}\\ &= \gamma\alpha_1 + (1-\gamma)\alpha_2\\ &\quad - \frac{\gamma(1-\gamma)(\alpha_1-\alpha_2)^2}{(1-\gamma)\alpha_1 + \gamma\alpha_2 - \alpha_3},\end{aligned} \tag{1.5}$$

as the parameter γ varies along the real axis in the interval $[0, 1]$.

2. Bounds on the complex bulk modulus of the composite

To find the bounds we use the following statement that was proved by Gibiansky and Milton (1993):

Statement A: The effective bulk modulus of the two-phase composite with *prescribed* volume fractions f and $(1-f)$ of the first and the second phases, respectively is shown to be constrained to a lens-shaped region in the complex bulk modulus plane bounded by the outermost pair of four circular arcs

$$\begin{aligned}\kappa^{(n)}(f,\gamma) &= f\kappa_1 + (1-f)\kappa_2\\ &\quad - \frac{f(1-f)(\kappa_1-\kappa_2)^2}{(1-f)\kappa_1 + f\kappa_2 + y^{(n)}(\gamma)},\\ &\qquad n = 1, 2, 3, 4.\end{aligned} \tag{2.1}$$

Here $f \in [0, 1]$ is fixed, γ varies along the real axis in the interval $[0, 1]$ and the functions $y^{(n)}(\gamma)$ are given by the formulas

$$y^{(1)}(\gamma) = \frac{4}{3}(\gamma\mu_1 + (1-\gamma)\mu_2), \tag{2.2}$$

$$y^{(2)}(\gamma) = \frac{4}{3}(\gamma/\mu_1 + (1-\gamma)/\mu_2)^{-1}, \tag{2.3}$$

$$\begin{aligned}y^{(3)}(\gamma) &= -\kappa_1\\ &\quad + [(4\mu_1/3 + \kappa_1)(4\mu_2/3 + \kappa_1)]\\ &\quad \times [\gamma(4\mu_2/3 + \kappa_1)\\ &\quad + (1-\gamma)(4\mu_1/3 + \kappa_1)]^{-1},\end{aligned} \tag{2.4}$$

$$\begin{aligned}y^{(4)}(\gamma) &= -\kappa_2\\ &\quad + [(4\mu_1/3 + \kappa_2)(4\mu_2/3 + \kappa_2)]\end{aligned}$$

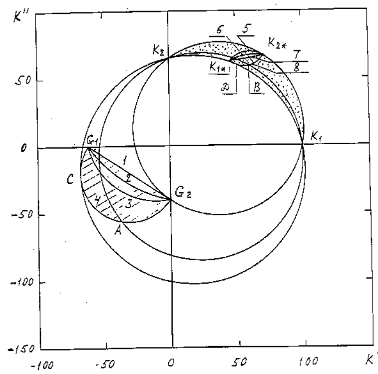

Fig. 1. The bounds for the bulk modulus of an isotropic composite of two isotropic phases, $\kappa_1 = 100$, $\mu_1 = 46$ and $\kappa_2 = i65$, $\mu_2 = i30$. (The following notation is used: $G_1 = -4\mu_1/3$, $G_2 = -4\mu_2/3$, $C = -y_1(\widehat{\gamma}_*)$, $D = \kappa^{(1)}(f, \widehat{\gamma}_*)$; left-hashed denotes $\widehat{G}_f(\kappa)$, $\kappa_* \in \widehat{G}_f(\kappa)$ for given f; dotted denotes $\widehat{G}(\kappa)$, $\kappa_* \in \widehat{G}(\kappa)$ for arbitrary f; right-hashed denotes Y.

$$\times[\gamma(4\mu_2/3 + \kappa_2) + (1-\gamma)(4\mu_1/3 + \kappa_2)]^{-1}. \tag{2.5}$$

One can check (see Appendix) that the above description is equivalent to the one given in the original paper and that the lines 2.1 (f is fixed, $\gamma \in [0,1]$) are really the arcs in the complex bulk modulus plane. These arcs are plotted in Fig. 1 and are denoted there as curve 5 (arc (2.1) $n = 1$), curve 6 (arc (2.1) $n = 3$), curve 7 (arc (2.1) $n = 4$), and curve 8 (arc (2.1) $n = 2$). For a fixed volume fraction $f = 0.5$ the bulk modulus κ_* is confined to the set $\widehat{G}_f(\kappa)$ bounded by the outermost of the arcs (2.1), $n = 1,2,3,4$. While f changes in the interval $[0, 1]$ this set draws the region $\widehat{G}(\kappa)$. For this example the bound of the $\widehat{G}(\kappa)$ set is drawn by the angular point κ_{2*} of the set $\widehat{G}_f(\kappa)$ and by the internal point D of arc 8. For any fixed $\gamma = \gamma_*$ the set of values of the function $\kappa^{(2)}(f, \gamma_*)$, while $f \in [0, 1]$, is $\text{Arc}(\kappa_1, \kappa_2, A)$, $A = -y^{(2)}(\gamma_*)$. It is drawn by the point $B = \kappa^{(2)}(f, \gamma_*)$ while f goes from zero to one. To find the bounds we draw the lines $\text{Arc}(G_1, G_2, \infty)$ (curve 1), $\text{Arc}(G_1, G_2, 0)$ (curve 4), Arc (G_1, G_2, κ_1) (curve 2), and Arc (G_1, G_2, κ_2) (curve 3). The bounds of $\widehat{G}(\kappa)$ set are given by $\text{Arc}(\kappa_1, \kappa_2, C)$ and $\text{Arc}(\kappa_1, \kappa_2, G_2)$ of two circles. The first of them contains the set Y, the other one has only one common point G_2 with it.

Note that all four arcs (2.1) intersect at the points

$$\kappa_{1*} = \kappa_1 + \frac{(1-f)}{1/(\kappa_2-\kappa_1) + 3f/(3\kappa_1 + 4\mu_1)}$$
$$= f\kappa_1 + (1-f)\kappa_2 - \frac{f(1-f)(\kappa_1-\kappa_2)^2}{(1-f)\kappa_1 + f\kappa_2 + 4\mu_1/3} \tag{2.6}$$

and

$$\kappa_{2*} = \kappa_2 + \frac{f}{1/(\kappa_1-\kappa_2) + 3(1-f)/(3\kappa_2 + 4\mu_2)}$$
$$= f\kappa_1 + (1-f)\kappa_2 - \frac{f(1-f)(\kappa_1-\kappa_2)^2}{(1-f)\kappa_1 + f\kappa_2 + 4\mu_2/3}, \tag{2.7}$$

because $y^{(n)}(0) = 4\mu_2/3$, $y^{(n)}(1) = 4\mu_1/3$ for every $n = 1,2,3,4$, see (2.2)–(2.5). Arc (2.1), $n = 1$ when extended passes also through the point $\kappa_a = f_1\kappa_1 + f_2\kappa_2$ (where $\gamma = \infty$) and can be described as $\text{Arc}(\kappa_{1*}, \kappa_{2*}, \kappa_a)$. Similarly, arc (2.1), $n = 2$ when extended passes through the point $\kappa_h = (f_1/\kappa_1 + f_2/\kappa_2)^{-1}$ (where $\gamma = \infty$) and can be described as $\text{Arc}(\kappa_{1*}, \kappa_{2*}, \kappa_h)$. Arcs (2.1), $n = 3,4$ when extended pass through the points κ_1 and κ_2, respectively (where $\gamma = \infty$). They can be described as $\text{Arc}(\kappa_{1*}, \kappa_{2*}, \kappa_1)$ and $\text{Arc}(\kappa_{1*}, \kappa_{2*}, \kappa_2)$.

We denote as $\widehat{G_f}(\kappa)$ the lens-shape region that is defined by the outermost pair of the arcs (2.1) (see Fig. 1 where the set $\widehat{G_f}(\kappa)$ is drawn and lines 5–8 represent the arcs (2.1)). Statement A means that this set contains the set $G_f(\kappa)$. If

we change the parameter f in the interval $[0, 1]$ this set changes its position in the complex bulk modulus plane (see Fig. 1) and covers the region $\widehat{G}(\kappa)$, $\widehat{G}(\kappa) = \cup_{f\in[0,1]}\widehat{G_f}(\kappa)$.

It is clear that $G(\kappa) \subset \widehat{G}(\kappa)$, i.e., this union contains the set $G(\kappa)$ and gives us the desirable bound on the complex bulk modulus of the composite with arbitrary volume fractions of the phases. The boundary points of the set $\widehat{G}(\kappa)$ are formed by the boundary points of the sets $\widehat{G_f}(\kappa)$ for some values of the parameter f, i.e., they can be described by the formula (2.1) for some $n = 1,2,3,4$, $f \in [0,1]$, and $\gamma \in [0,1]$. To find the desirable bounds we find the track that each of the arcs (2.1), $\gamma \in [0,1]$ draws while f varies from zero to one. The union of all such tracks gives us the set $\widehat{G}(\kappa)$ (see Fig. 1).

Let us first formulate the result and then give the explanation. It turns out that the bounds can be described in the pure geometrical way. In what follows we refer to Fig. 1 where the values of the moduli are chosen as $\kappa_1 = 100$, $\mu_1 = 46$, $\kappa_2 = i65$, and $\mu_2 = i30$. Such values of the moduli look artificial but we chose them only because they are convenient for the illustration disposition of all circles and arcs that we use in the procedure of constructing the bounds.

Namely, to find the bounds we should do the following. First, we put on the complex bulk modulus plane the points κ_1, κ_2, $G_1 = -4\mu_1/3$, and $G_2 = -4\mu_2/3$ and denote as 0 the origin and as ∞ the infinity points of this plane. Then we draw the lines $\text{Arc}(G_1, G_2, \infty)$ (it is the straight line connecting the points G_1 and G_2, curve 1 in Fig. 1), Arc $(G_1, G_2, 0)$ (curve 4), $\text{Arc}(G_1, G_2, \kappa_1)$ (curve 2), and $\text{Arc}(G_1, G_2, \kappa_2)$ (curve 3). Comparing (1.5) and (2.2)–(2.5) one can see that these arcs are the sets of the values of the functions $-y^{(n)}(\gamma)$, $n = 1,2,3,4$ respectively while $\gamma \in [0,1]$. Let denote as Y the set defined by the outermost pair of these four arcs. These arcs 1, 2, 3, 4 and the set Y have no immediate physical meaning although they play an important role in the procedure that we describe. The bounds on the complex bulk modulus of the composite with arbitrary volume fractions of the phases are given by two arcs ($\text{Arc}(\kappa_1, \kappa_2, C)$ and $\text{Arc}(\kappa_1, \kappa_2, G_2)$ in Fig. 1). They pass through the points κ_1 and κ_2 of the original materials and when extended to circles touch the set Y. One of these circles (circle κ_1–C–κ_2 in Fig. 1) contains this set, the other one (circle κ_1–G_2–κ_2 in Fig. 1) has only one common point with it.

Indeed, as we show, to define the bounds we need to find the union of the sets of the values for the functions $\kappa^{(n)}(f, \gamma)$, $n = 1,2,3,4$ while $f \in [0,1]$, $\gamma \in [0,1]$. For any fixed $\gamma = \gamma_*$ the set of the values of the function $\kappa^{(n)}(f, \gamma_*)$, $f \in [0,1]$ is $\text{Arc}(\kappa_1, \kappa_2, -y^{(n)}(\gamma_*))$, compare (1.5) and (2.1). (In Fig. 1 see $\text{Arc}(\kappa_1, \kappa_2, A)$, $A = -y^{(2)}(\gamma_*)$ that is drawn by the point $B = \kappa^{(2)}(f, \gamma_*)$ while f goes from zero to one.) The union over $\gamma_* \in [0,1]$ of all such arcs defines the track of the corresponding arc (2.1). By repeating the same procedure for all $n = 1,2,3,4$ we clearly end up with the bounds described above.

In other words, any arc that is described by (2.1), $f \in [0,1]$, for some n and some γ_*, passes through the points κ_1 and κ_2 and when extended crosses the Y set. The bounds are given by the outermost pair of all these arcs.

Note the two possible variants how the boundary circle may touch the Y set. It may pass through one of the corner points of this set, say $G_2 = -4\mu_2/3$ as in Fig. 1. In this case the corresponding bound of the set $\widehat{G}(\kappa)$ is drawn by the corner point κ_{2*} of the set $\widehat{G_f}$. The boundary circle may also touch the set Y in some internal point C of their boundary arc. Then the arc of this circle connecting the points κ_1 and κ_2 is drawn by the internal point D of the boundary arc of the set $\widehat{G_f}$, see Fig. 1.

Although the description of the results is simple, it is not so easy to find the exact formulas. Here we give the results, the reader can find the details and calculations in the Appendix. To find the bounds on the effective complex bulk modulus we should first calculate the values γ_*, γ_{**}, $\widehat{\gamma}_*$ and $\widehat{\gamma}_{**}$ by using the formulas

$$\gamma_* = \frac{-B_1 + \sqrt{B_1^2 - 4A_1C_1}}{2A_1},$$

$$\gamma_{**} = \frac{-B_1 - \sqrt{B_1^2 - 4A_1C_1}}{2A_1},$$

$$\text{if} \quad D_1 = B_1^2 - 4A_1C_1 \ge 0, \quad A_1 \ne 0;$$

$$\gamma_* = \gamma_{**} = -C_1/B_1, \quad \text{if} \quad A_1 = 0;$$

$$\gamma_* \ \text{and} \ \gamma_{**} \ \text{are undefined}$$

$$\text{if} \quad D_1 < 0, \tag{2.8}$$

where

$$A_1 = \frac{4}{3}\left(\frac{\mu_1 - \mu_2}{\kappa_1 - \kappa_2}\right)'',$$

$$B_1 = \left(\frac{\kappa_1 + \kappa_2 + 8\mu_2/3}{\kappa_1 - \kappa_2}\right)'',$$

$$C_1 = \left(\frac{(3\kappa_1/4 + \mu_2)(\kappa_2 + 4\mu_2/3)}{(\kappa_1 - \kappa_2)(\mu_1 - \mu_2)}\right)'', \tag{2.9}$$

and

$$\hat{\gamma}_* = \frac{-B_2 + \sqrt{B_2^2 - 4A_2C_2}}{2A_2},$$

$$\hat{\gamma}_{**} = \frac{-B_2 - \sqrt{B_2^2 - 4A_2C_2}}{2A_2},$$

$$\text{if} \quad D_2 = B_2^2 - 4A_2C_2 \ge 0, \quad A_2 \ne 0;$$

$$\hat{\gamma}_* = \hat{\gamma}_{**} = -C_2/B_2, \quad \text{if} \quad A_2 = 0;$$

$$\hat{\gamma}_* \ \text{and} \ \hat{\gamma}_{**} \ \text{are undefined}$$

$$\text{if} \quad D_2 < 0, \tag{2.10}$$

where

$$A_2 = \left(\frac{3(1/\mu_1 - 1/\mu_2)}{4(1/\kappa_1 - 1/\kappa_2)}\right)'',$$

$$B_2 = \left(\frac{[1/\kappa_1 + 1/\kappa_2 + 3/(2\mu_2)]}{(1/\kappa_1 - 1/\kappa_2)}\right)'',$$

$$C_2 = \{(4/(3\kappa_1) + 1/\mu_2)[1/\kappa_2 + 3/(4\mu_2)] \times [(1/\kappa_1 - 1/\kappa_2) \times (1/\mu_1 - 1/\mu_2)] - 1\}''. \tag{2.11}$$

Then on the complex bulk modulus plane we should enscribe

$$\mathrm{Arc}(\kappa_1, \ \kappa_2, \ -4\mu_1/3),$$

$$\mathrm{Arc}(\kappa_1, \ \kappa_2, \ -4\mu_2/3),$$

$$\mathrm{Arc}(\kappa_1, \ \kappa_2, \ -y^{(1)}(\gamma_*)), \quad \text{if} \quad \gamma_* \in [0,1],$$

$$\mathrm{Arc}(\kappa_1, \ \kappa_2, \ -y^{(1)}(\gamma_{**})), \quad \text{if} \quad \gamma_{**} \in [0,1],$$

$$\mathrm{Arc}(\kappa_1, \ \kappa_2, \ -y^{(2)}(\hat{\gamma}_*)), \quad \text{if} \quad \hat{\gamma}_* \in [0,1]$$

and

$$\mathrm{Arc}(\kappa_1, \ \kappa_2, \ -y^{(2)}(\hat{\gamma}_{**})), \quad \text{if} \quad \hat{\gamma}_{**} \in [0,1].$$

The outermost pair of these arcs gives us the bounds of the $\widehat{G}(\kappa)$ set, that were described above, see Fig. 1.

3. The microstructures that possess the extremal complex bulk modulus

The natural way to check whether the obtained bounds are exact is to try to find the microstructures that possess the extremal properties in the sense that their bulk modulus corresponds to the bounds. In this section we describe such structures with the bulk modulus that lies on the boundary of the $\widehat{G}(\kappa)$ set. Because any of the arcs (2.1) may form the bound it is interesting to find the structures corresponding to the points on all of these lines. In order to use the results on the effective properties of the elastic structures we recall the correspondence principle, see for example Hashin (1970): "The effective complex moduli of a viscoelastic composite are obtained by replacement of phase elastic moduli by corresponding phase viscoelastic complex moduli in the expressions for effective elastic moduli of an elastic composite with identical phase geometry".

First we note that the expression (2.6) for the $\mathrm{Arc}(\kappa_1, \kappa_2, -4\mu_1/3)$ for any fixed value of the parameter f gives the effective bulk modulus of an assemblage of the Hashin–Shtrikman coated spheres (see Hashin and Shtrikman (1963)) with the inclusions of the second material into the matrix of the first one. Therefore each point on this arc corresponds to the effective bulk modulus of the Hashin–Shtrikman coated spheres assemblage for some volume fraction f of the first phase. Similarly each point on the arc $\mathrm{Arc}(\kappa_1, \kappa_2, -4\mu_1/3)$ (see expression (2.7)) corresponds to the Hashin–Shtrikman coated spheres assemblage with the inclusions of the first material into the matrix of the second one. Hence if any of these arcs forms the bound this bound is exact because there exists composite material that corresponds to any point on that part of the boundary.

As to the other possible boundary arcs, only several points on these lines correspond to some known structures. As was shown by Gibiansky and Milton (1993) there exist composites that possess bulk moduli $\kappa_b^{(1)}$, $\kappa_b^{(2)}$, $\kappa_b^{(3)}$, and $\kappa_b^{(4)}$ such that

$$\kappa_b^{(n)}(f) = f\kappa_1 + (1-f)\kappa_2 - \frac{f(1-f)(\kappa_1 - \kappa_2)^2}{(1-f)\kappa_1 + f\kappa_2 + y_b^{(n)}(f)},$$

$$n = 1,2,3,4, \tag{3.1}$$

where

$$y_b^{(1)}(f) = \frac{4}{3}\left(\frac{f}{\mu_2} + \frac{(1-f)}{\mu_1}\right)^{-1},$$

$$y_b^{(2)}(f) = \frac{4}{3}(f\mu_2 + (1-f)\mu_1), \tag{3.2}$$

$$y_b^{(3)}(f) = \frac{(4-f)\mu_1}{3} + \frac{f\mu_2}{3},$$

$$y_b^{(4)}(f) = \frac{(1-f)\mu_1}{3} + \frac{(3+f)\mu_2}{3}. \tag{3.3}$$

We do not recall the description of these structures here, the reader can find the details in the original paper.

If $\gamma = \gamma_*$ or $\gamma = \gamma_{**}$ (see (2.8) and (2.9)) belongs to the interval $[0,1]$ then the structures $\kappa_b^{(2)}, \kappa_b^{(3)}$, and $\kappa_b^{(4)}$ lie on the arc $\kappa^{(1)}(f, \gamma)$ when

$$f = f_b^{(2)} = 1 - \gamma,$$

$$f = f_b^{(3)} = 4(1 - \gamma),$$

$$f = f_b^{(4)} = 1 - 4\gamma, \tag{3.4}$$

respectively. We should however check whether the volume fractions defined by (3.4) lie in the interval $[0,1]$. It is always true for the composite $\kappa_b^{(2)}$, but it gives some restrictions on values γ for the composite $\kappa_b^{(3)}$ (namely, $f_b^{(3)} \in [0,1]$ when $\gamma \in [3/4,1]$) and for the composite $\kappa_b^{(4)}$ ($f_b^{(4)} \in [0,1]$ when $\gamma \in [0,1/4]$). In summary, only two attainable points $\kappa_b^{(2)}$ and $\kappa_b^{(4)}$ are known on the boundary arc $\kappa^{(1)}(f, \gamma)$ ($\gamma = \gamma_*$ or $\gamma = \gamma_{**}$ is fixed, $f \in [0,1]$) if $\gamma \in [0,1/4]$, only one such point $\kappa_b^{(2)}$ is known if $\gamma \in [1/4,3/4]$, and only two such points $\kappa_b^{(2)}$ and $\kappa_b^{(3)}$ are known if $\gamma \in [3/4,1]$.

If $\gamma = \hat{\gamma}_*$ or $\gamma = \hat{\gamma}_{**}$ (see (2.10) and (2.11)) belongs to the interval $[0,1]$ then the structure with the bulk modulus $\kappa_b^{(1)}$ lies on the arc $\kappa^{(2)}(f, \gamma)$ when

$$f = f_b^{(1)} = 1 - \gamma. \tag{3.5}$$

We can also use the results of the second section to obtain the bounds for the properties of an anisotropic composite. First note, that for every anisotropic viscoelastic material with the viscoelasticity tensor C there exists an isotropic polycrystal microstructure that possesses the bulk modulus

$$\kappa^{\mathrm{V}}(C) = \frac{1}{3}I : CI = \frac{1}{3}\sum_{i,j=1}^{3} C_{iijj} \tag{3.6}$$

and a polycrystal that possesses the bulk modulus (see Avellaneda and Milton (1989), Rudelson (1989), Gibiansky and Milton (1993)).

$$\kappa^{\mathrm{R}}(C) = 3(I : C^{-1}I)^{-1} = 3\left(\sum_{i,j=1}^{3}(C^{-1})_{iijj}\right)^{-1}. \tag{3.7}$$

Here I is a unit matrix, double dots denote the scalar product, C_{iijj} and $(C^{-1})_{iijj}$ are the elements of the tensors C and C^{-1}, respectively, in the Cartesian basis. Indices V and R refer to the fact that the expressions (3.6) and (3.7) coincide with the Voigt and Reuss bounds on the effective bulk modulus of an isotropic elastic polycrystal prepared from a monocrystal with the elasticity tensor C. Therefore for any anisotropic two-phase viscoelastic composite C the quantities $\kappa^{\mathrm{V}}(C)$ and $\kappa^{\mathrm{R}}(C)$ that measure the reaction of the composite on the bulk-type stress or strain field should satisfy the restrictions of the second section for the bulk modulus of the isotropic composite. Indeed, we can always prepare from it two isotropic polycrystals with the bulk moduli $\kappa^{\mathrm{V}}(C)$ and $\kappa^{\mathrm{R}}(C)$ respectively that should lie within the bounds of the second section. The same arguments were used by Gibiansky and Milton (1993) to apply the bounds on bulk modulus to anisotropic composites.

4. Some particular cases and discussion

In this section we implement the obtained results to study the composite made of particular phases. We plot these bounds and discuss the results of numerical calculations.

4.1. Composite of the stiff purely elastic phase and the soft phase with high damping

Figure 2 shows the numerically obtained bounds for the composite material, prepared from the stiff purely elastic phase with moduli $\kappa_1 = 100$, $\mu_1 = 46$ and the soft phase with high damping in shear with moduli $\kappa_2 = 0.5$, $\mu_2 = 0.5 + \mathrm{i}1.5$. The lower bound (curve 1 that coincide here with the interval of the real axis) is exact and corresponds to the assemblages of Hashin–Shtrikman coated spheres where the stiff elastic phase forms the matrix and the soft dissipative phase is placed into the inclusions. The dissipation rate on this curve is equal to zero. Indeed, in the average hydrostatic strain or stress field the local fieli in the inclusions is also hydrostatic for

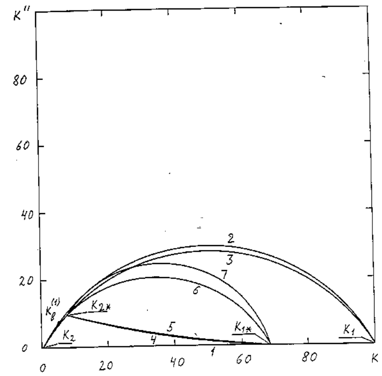

Fig. 2. The bounds for the bulk modulus of an isotropic composite of the stiff elastic phase $\kappa_1 = 100$, $\mu_1 = 46$ and the soft viscoelastic phase $\kappa_2 = 0.5$, $\mu_2 = 0.5 + \mathrm{i}1.5$.

these structures. Therefore there is no dissipation because it can occur only in shear deformation of the second phase, in this example. The upper bound (curve 2) has only one point $\kappa_b^{(1)}$ that is known to be attainable. Curve 3 corresponds to the Hashin–Shtrikman structures where the stiff inclusions of the first phase are surrounded by the soft second phase. The outermost pair of the internal arcs 4, 5, 6, 7 forms the bounds for the bulk modulus of a composite with fixed volume fraction $f = 0.85$ of the first phase. It is interesting to observe that the soft phase can contribute so much into the whole dissipation of the composite. This fact have been known for a long time and may be explained by the high concentration of the field in the soft phase. This is consistent with the results of Chen and Lakes (1993).

4.2. Composite of the phases that possess equal and real Poisson's ratios

The expressions for the bounds can be greatly simplified if we assume that the original materials possess real and equal Poisson's ratios $\nu_1 = \nu_2 = \nu$, $\nu'' = 0$. In this case

$$\mu_1 = c\kappa_1, \qquad \mu_2 = c\kappa_2,$$

$$c = \frac{3(1-2\nu)}{2(1+\nu)}, \tag{4.1}$$

where c is a real number. It immediately follows from (2.8), (2.9) and (4.1) that

$$A_1 = 4c''/3 = 0,$$

$$B_1 = \left(\frac{\kappa_1 + \kappa_2 + 8c\kappa_2/3}{\kappa_1 - \kappa_2}\right)'' = \frac{2(3+4c)}{3}\left(\frac{\kappa_2}{\kappa_1 - \kappa_2}\right)'', \tag{4.2}$$

$$C_1 = \left(\frac{(3+4c)\kappa_2(3\kappa_1 + 4c\kappa_2)}{12c(\kappa_1-\kappa_2)^2}\right)'' = \frac{3+4c}{4c}\left[\left(\frac{\kappa_2}{\kappa_1-\kappa_2}\right) + \frac{3+4c}{3}\left(\frac{\kappa_2}{\kappa_1-\kappa_2}\right)^2\right]'', \tag{4.3}$$

$$\gamma_* = -C_1/B_1 = -\frac{3}{8c} - \frac{3+4c}{4c}\left(\frac{\kappa_2}{\kappa_1-\kappa_2}\right)'. \tag{4.4}$$

To get the last relationship we use the equality $(a^2)''/a'' = [(a' + \mathrm{i}a'')^2]''/a'' = 2a'$. As we see, parameter γ_* depends only on the parameter $R = [\kappa_2/(\kappa_1 - \kappa_2)]'$.

Similarily from (2.10) and (2.11) we deduce

$$\widehat{\gamma}_* = -\frac{2c}{3} - \frac{3+4c}{3}\left(\frac{1/\kappa_2}{1/\kappa_1 - 1/\kappa_2}\right)' = \frac{3+2c}{3} + \frac{3+4c}{3}\left(\frac{\kappa_2}{\kappa_1-\kappa_2}\right)'. \tag{4.5}$$

One can verify that

$$\text{if} \quad R \in \left[-\frac{3+8c}{6+8c}, -\frac{3}{6+8c}\right], \quad \text{then} \quad \gamma_* \in [0,1] \tag{4.6}$$

and

$$\text{if} \quad R \in \left[-\frac{3+2c}{3+4c}, -\frac{2c}{3+4c}\right], \quad \text{then} \quad \widehat{\gamma}_* \in [0,1]. \tag{4.7}$$

Therefore to find the bounds on the effective complex bulk modulus of the composite of two phases with equal and real Poisson's ratios we need to calculate two quantities γ_* and $\widehat{\gamma}_*$ by formulas (4.4) and (4.5). In the bulk modulus plane we need to enscribe the arcs

$$\mathrm{Arc}(\kappa_1, \kappa_2, -4\mu_1/3),$$

$$\mathrm{Arc}(\kappa_1, \kappa_2, -4\mu_2/3),$$

$$\mathrm{Arc}(\kappa_1, \kappa_2, -y^{(1)}(\gamma_*)), \quad \text{if} \quad \gamma_* \in [0,1]$$

and

$$\mathrm{Arc}(\kappa_1, \kappa_2, -y^{(2)}(\widehat{\gamma}_*)), \quad \text{if} \quad \widehat{\gamma}_* \in [0,1].$$

The outermost pair of these four, three or two arcs forms bounds on $\widehat{G}(\kappa)$ set, i.e., on complex bulk modulus of the composite.

Figures 3 and 4 show the numerical results that describe the dependence of the bounds on the Poisson's ratio of phases. We use here, instead of the bulk modulus plane, the stiffness loss map, where the absolute value $|\kappa|$ of the bulk modulus is plotted versus the loss tangent κ''/κ', to present the results. These coordinates are more usual for the applications. First (see Fig. 3) we take the phases with the bulk moduli $\kappa_1 = 100 + \mathrm{i}0.1$, $\kappa_2 = 30 + \mathrm{i}30$ and the Poisson's ratio $\nu = -0.25$ (curves 1, 2), $\nu = 0$ (curves 3, 4), $\nu = 0.25$ (curves 5, 6), $\nu = 0.5$ (curves 7, 8). For these values of the parameters all bounds are exact and correspond to the Hashin–Shtrikman coated spheres. Increasing the Poisson's ratio of the phases results in increasing the dissipation. For the extreme value $\nu = 0.5$ the lower and upper bounds coincide and uniquely define the relation between the real and imaginary parts of the composite bulk modulus. Indeed, the value $\nu = 0.5$ for the fixed bulk moduli leads to zero shear moduli of the phases. For the composite made of such materials the properties are defined by the volume fractions of the phases (namely, $\kappa_* = (f/\kappa_1 + (1-f)/\kappa_2)^{-1}$) and are independent of the microstructure (see Christensen (1979), for example).

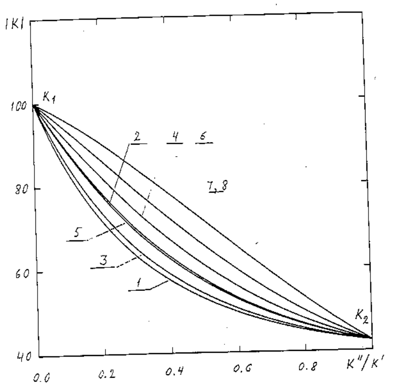

Fig. 3. The bounds for the bulk modulus of a composite of phases with the bulk moduli $\kappa_1 = 100 + i0.1$ and $\kappa_2 = 30 + i30$. The Poisson's ratios of the phases are real and equal $\nu = -0.25$ (curves 1, 2), $\nu = 0$ (curves 3, 4), $\nu_1 = 0.25$ (curves 5, 6), $\nu = 0.5$ (curves 7, 8). All bounds are exact and correspond to the assemblages of the Hashin–Shtrikman coated spheres.

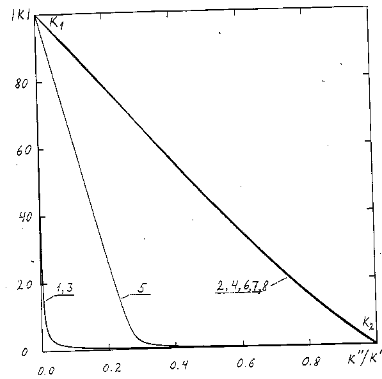

Fig. 4. The same as in Fig. 3 but $\kappa_1 = 100 + i0.1$, $\kappa_2 = 0.1 + i0.1$. $\nu = -0.25$ (curves 1, 2), $\nu = 0.25$ (curves 3, 4), $\nu = 0.499$ (curves 5, 6), $\nu = 0.5$ (curves 7, 8). Note that composite can have a higher value of κ''_* than either of components, but the loss tangent κ''_*/κ'_* of the composite can not exceed the loss tangent $\kappa''/\kappa' = \mu''/\mu'$ of either phase.

Figure 4 describes the results for the bulk moduli of the phases $\kappa_1 = 100+i0.1$, $\kappa_2 = 0.1+i0.1$ and the Poisson's ratio $\nu = -0.25$ (curves 1, 2), $\nu = 0.25$ (curves 3, 4), $\nu = 0.499$ (curves 5, 6), $\nu = 0.5$ (curves 7, 8). In these examples the upper bounds for all values of Poisson's ratio practically coincide whereas the lower bounds differ only in a very narrow interval around $\nu = 0.5$. All these bounds are also exact and correspond to the Hashin–Shtrikman structures.

4.3. *Dependence of the bounds on the Poisson's ratios of the phases*

If the constituents have real but unequal Poisson's ratios, the bounds are shifted as shown in Fig. 5 for the bulk moduli of the phases $\kappa_1 = 100 + i0.1$, $\kappa_2 = 30 + i30$ and the Poisson's ratios $\nu_1 = 0.1$, $\nu_2 = 0.5$ (curves 1, 8), $\nu_1 = 0.2$, $\nu_2 = 0.4$ (curves 2, 7), $\nu_1 = \nu_2 = 0.3$ (curves 3, 6), and $\nu_1 = 0.39$, $\nu_2 = 0.21$ (curves 4, 5). The structures corresponding to these curves are the assemblages of the Hashin–Shtrikman coated spheres, in which the spherical inclusions of the second phase are surrounded by the matrix of the first phase (for the curves 1, 2, 3, and 4, that are the lower bounds) or vise versa, the inclusions of the first phase are embedded into the matrix of the second phase (curves 5, 6, 7, and 8, that are the upper bounds). For the Hashin–Shtrikman coated spheres assemblages the bulk modulus of the composite does not depend on the shear modulus of the inclusions, i.e., in our case it does not depend on the Poisson's ratio ν_2 for the lower bounds 1, 2, 3, and 4 and on the Poisson's ratio ν_1 for the upper bounds 5, 6, 7, and 8. An increase in the Poisson's ratio of the matrix material leads to the increase of the dissipation rate of the composite, as can be seen on both upper and lower bounds.

We also consider the composites made of the phases with the complex values of the Poisson's ratios. The complex Poisson's ratios of the phases influence the bounds as shown in Fig. 6 for the bulk moduli of phases $\kappa_1 = 100+i0.1$, $\kappa_2 =$

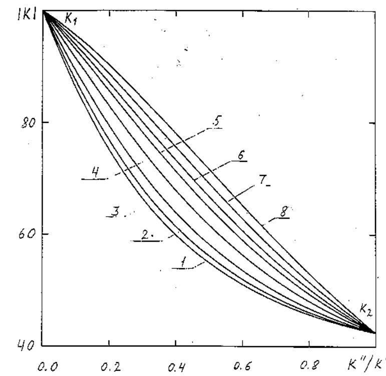

Fig. 5. The bounds for the composite of phases with the bulk moduli $\kappa_1 = 100 + i0.1$ and $\kappa_2 = 30 + i30$. The Poisson's ratios of the phases are real and $\nu_1 = 0.1$, $\nu_2 = 0.5$ (curves 1, 8), $\nu_1 = 0.2$, $\nu_2 = 0.4$ (curves 2, 7), $\nu_1 = \nu_2 = 0.3$ (curves 3, 6), and $\nu_1 = 0.39$, $\nu_2 = 0.21$ (curves 4, 5). The bounds are exact and correspond to the assemblages of the Hashin–Shtrikman coated spheres.

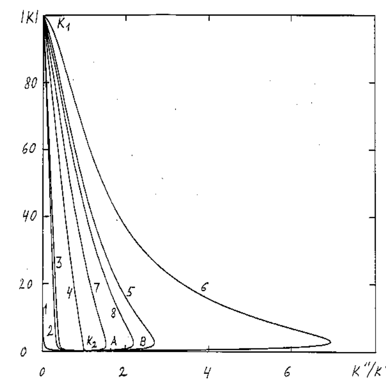

Fig. 6. The bounds for the composite of phases with the bulk moduli $\kappa_1 = 100 + i0.1$ and $\kappa_2 = 0.1 + i0.1$.

$0.1+i0.1$ and equal Poisson's ratios $\nu_1 = \nu_2 = \nu$ and $\nu = 0.3$ (curves 1, 4), $\nu = 0.3\exp(-i0.12\pi)$ (curves 2, 5), and $\nu = 0.3\exp(-i0.225\pi)$ (curves 3, 6). A negative argument of the complex Poisson's ratio corresponds to higher dissipation on the shear deformations comparing with the hydrostatic deformation of the material. The bounds 1, 2, 3, and 4 correspond to the Hashin–Shtrikman structures and therefore are exact, the points A (on curve 5) and B (on curve 6) also are attainable and correspond to the composite $\kappa_b^{(1)}$, see (3.1), (3.3). Curves 7 and 8 correspond to the Hashin–Shtrikman structures for

$$\nu = 0.3\exp(-i0.12\pi) \quad \nu = 0.3\exp(-i0.225\pi),$$

respectively.

One can see that the loss tangent κ''_*/κ'_* of the composite can be greater than the loss tangent of either phase. However, there are two independent moduli (e.g., bulk and shear) and one can prove that the loss tangent associated with the bulk modulus of the composite can be no larger than the maximal and no smaller than the minimal loss tangent (for the bulk or shear deformations) of either phase, i.e.,

$$\min\,[\kappa''_1/\kappa'_1,\ \kappa''_2/\kappa'_2,\ \mu''_1/\mu'_1,\ \mu''_2/\mu'_2] \le \kappa''_*/\kappa'_* \le \max[\kappa''_1/\kappa'_1,\ \kappa''_2/\kappa'_2,\ \mu''_1/\mu'_1,\ \mu''_2/\mu'_2]. \quad (4.8)$$

It is clear because the average dissipation rate of the composite cannot be smaller than minimal or larger than maximal dissipation rate of the phases. The upper bound 6 that allows the composites with a high dissipation rate is similar to the one described by Fig. 3. Indeed, such choice of the Poisson's ratio leads to a very small real part of the shear modulus of the second material. Together with the choice of the bulk moduli it guarantees the opportunity of the high dissipation.

4.4. *Conclusions*

In summary, in this paper we obtained the visual geometrical description and the explicit formulas for the bounds on the complex bulk modulus of the viscoelastic two-phase composite with arbitrary volume fractions of the phases. The bounds have particularly simple form when the phases have equal and real Poisson's ratios. The bounds were analyzed in order to find the conditions that give rise to the dissipation rate of the composite. In particular, the known experimental fact that small amount of dissipative inclusions in a stiff matrix may dramatically increase the whole dissipation rate of the composite agrees with our bounds, as can be seen in Fig. 2. The dependence of the bounds on the Poisson's ratios of the phases was analyzed numerically, the results are summarized in Figs. 3–6. The structures that correspond to the various parts of the bounds were identified. Therefore at least some parts of the obtained bounds are exact, they are attainable by the assemblages of Hashin–Shtrikman coated spheres. The rest of the bounds are rather restrictive although it is not known whether they can be improved or not.

Acknowledgements

We are pleased to thank A.V. Cherkaev and G.W. Milton for helpful discussions and suggestions that improved the manuscript.

References

Avellaneda, M. (1987), Optimal bounds and microgeometries for elastic two-phase composites, *SIAM J. Appl. Math. 47*, 1216.

Avellaneda, M. and G.W. Milton (1989), Optimal bounds on the effective bulk modulus of polycrystals, *SIAM J. Appl. Math. 49*, 824.

Chen, C.P. and R.S. Lakes (1993), Analysis of high loss viscoelastic composites, *J. Math. Sci. 28*, in press.

Cherkaev, A.V. and L.V. Gibiansky (1992), The exact coupled bounds for effective tensors of electrical and magnetic properties of two-component two-dimensional composites, *Proc. R. Soc. Edinburgh 122 A*, 93–125.

Cherkaev, A.V. and L.V. Gibiansky (1993a), Coupled estimates for the bulk and shear moduli of a two-dimensional isotropic elastic composite, *J. Mech. Phys. Solids 41(5)*, 937–980.

Cherkaev, A.V. and L.V. Gibiansky (1993b), Variational principles for complex conductivity, viscoelasticity and similar problems for media with complex moduli, *J. Math. Phys.*, submitted to.

Christensen, R.M. (1969), Viscoelastic properties of heterogeneous media, *J. Mech. Phys. and Solids 17*, 23.

Christensen, R.M. (1971), *Theory of Viscoelasticity*, Academic Press, New York.

Christensen, R.M. (1979), *Mechanics of Composite Materials*, Wiley-Interscience, New York.

Gibiansky, L.V. and G.W. Milton W. (1993), On the effective viscoelastic moduli of two-phase media: I. Rigorous bounds on the complex bulk modulus, *Proc. R. Soc. London A440*, 163–188.

Hashin, Z. (1965), Viscoelastic behaviour of heterogeneous media, *ASME J. Appl. Mech. 32*, 630.

Hashin, Z. (1970), Complex moduli of an viscoelastic composites: I General theory and application to particulate composites, *Int. J. Solids Struct. 6*, 539.

Hashin, Z. and S. Shtrikman (1963), A variational approach to the theory of the elastic behaviour of multiphase materials, *J. Mech. Phys. Solids 11*, 127.

Kohn, R.V. and G.W. Milton (1988), Variational bounds on the effective moduli of anisotropic composites, *J. Mech. Phys. Solids 36(6)*, 597.

Lurie, K.A. and A.V. Cherkaev (1986), The effective characteristics of composite materials and optimal design of constructions, *Adv. Mech. (Poland) 9(2)*, 3.

Milton, G.W. (1981), Bounds on the complex permittivity of a two-component composite material, *J. Appl. Phys. 52(8)*, 5286.

Milton, G.W. (1990), On characterizing the set of possible effective tensors of composites: The variational method and the translation method, *Comm. Pure Appl. Math. XLIII*, 63.

Roscoe, R. (1969), Bounds for real and imaginary parts of the dynamic moduli of composite viscoelastic system, *J. Mech. Phys. Solids 17*, 17.

Roscoe, R. (1972), Improved bounds for real and imaginary parts of complex moduli of isotropic viscoelastic composites, *J. Mech. Phys. Solids 20*, 91.

Rudelson, M. (1989, Phase transitions in solids, Masters degree thesis, Leningrad Polytechnical Institute, Leningrad.

Appendix

(1) To obtain the bounds for the complex bulk modulus the special fraction linear transformation were used by Gibiansky and Milton (1993). This transformation $y(\kappa)$ is defined through the formula

$$\kappa = f\kappa_1 + (1-f)\kappa_2 - \frac{f(1-f)(\kappa_1-\kappa_2)^2}{(1-f)\kappa_1 + f\kappa_2 + y(\kappa)}, \tag{A.1}$$

or explicitly

$$y(\kappa) = y_f(\kappa,\kappa_1,\kappa_2) = -(1-f)\kappa_1 - f\kappa_2 + \frac{f(1-f)(\kappa_1-\kappa_2)^2}{f\kappa_1 + (1-f)\kappa_2 - \kappa}, \tag{A.2}$$

(see details and references in the original paper). Due to the one-to-one correspondence between κ_* and $y(\kappa_*)$ the bounds can be formulated in terms of $y(\kappa_*)$. As was proved by Gibiansky and Milton (1993), to find the bounds for the quantity $y(\kappa_*)$ one should in the $y(\kappa)$-plane inscribe a straight line $\mathrm{Arc}(4\mu_1/3,\ 4\mu_2/3,\ \infty)$ drawn between the points $4\mu_1/3 = 4\mu_1/3$ and $4\mu_2/3 = 4\mu_2/3$ and three arcs

$$\mathrm{Arc}(4\mu_1/3,\ 4\mu_2/3,\ 0),$$

$$\mathrm{Arc}(4\mu_1/3,\ 4\mu_2/3,\ -\kappa_1),$$

and

$$\mathrm{Arc}(4\mu_1/3,\ 4\mu_2/3,\ -\kappa_2).$$

The outermost pair of these lines gives us the bounds on $y(\kappa_*)$.

One can check (comparing (1.5) and (2.2)) that

$$\mathrm{Arc}(4\mu_1/3,\ 4\mu_2/3,\ \infty)$$

is described by formula (2.2). Indeed,

$$y^{(1)}(1) = 4\mu_1/3, \qquad y^{(1)}(0) = 4\mu_2/3,$$

and

$$y^{(1)}(\infty) = \infty.$$

Similarly, $\mathrm{Arc}(4\mu_1/3,\ 4\mu_2/3,\ 0)$ is described by the formula (2.3), $\mathrm{Arc}(4\mu_1/3,\ 4\mu_2/3,\ \kappa_1)$ is described by formula (2.4), and $\mathrm{Arc}(4\mu_1/3, 4\mu_2/3, \kappa_2)$ is described by the formula (2.5).

Inverse Y-transformation (defined by (A.1)) maps these arcs into the complex bulk modulus plane. Clearly, images of the arcs (2.2)–(2.5) are given by lines (2.1), $n = 1, 2, 3, 4$, respectively.

The Y-transformation is a fractional linear one. Therefore, it maps circle into circle and arc into arc. It means that the lines described by (2.1) are really the arcs on the complex bulk modulus plane. Therefore the bounds on the bulk modulus are given by the outermost pair of four arcs (2.1).

(2) As we mentioned before, the boundary points of the set $\widehat{G}(\kappa)$ are formed by the boundary points of the sets $\widehat{G_f}(\kappa)$ for some values of the parameter f. To find the desirable bounds we find the track that each of the arcs (2.1) draws while f varies from zero to one. The union of all these tracks gives us the set $\widehat{G}(\kappa)$, see Fig. 1.

There are two possible variants how any of the arcs (2.1) may form the bounds of its track. First, it may be drawn by one of the end points κ_{1*} or κ_{2*} of the arc (2.1) (like for the arcs $n = 1$, $n = 3$ and $n = 4$ on Fig. 1). It is easy to see from (1.5), (2.6) and (2.7) that lines drawn by these points are $\mathrm{Arc}(\kappa_1,\ \kappa_2,\ -4\mu_1/3)$ and $\mathrm{Arc}(\kappa_1,\ \kappa_2,\ -4\mu_2/3)$, respectively.

Secondly, it may be also drawn by the internal point of the arc (as for the arc (2.1) $n = 2$ in Fig. 1). Note that in this particular case the position of the internal point D is described by the formula (2.1), $n = 2$ for some $f \in [0,\ 1]$, $\gamma \in [0,\ 1]$, or in general by one of the formulas (2.1).

The outermost pair of all these lines gives us the bound for $\widehat{G}(\kappa)$ set (see Fig. 1).

Let us find the conditions that define the internal points that may draw the boundary lines for the tracks of the arcs (2.1).

Let us study some point $\kappa^{(n)}(f_*,\ \gamma_*)$. The small variation $\partial\kappa^{(n)}(f_*,\ \gamma_*)$ of the position of this point is given by

$$\begin{aligned}\delta\kappa^{(n)}(f_*,\ \gamma_*) &= \kappa^{(n)}(f_* + \delta f,\ \gamma_* + \delta\gamma) \\ &\quad - \kappa^{(n)}(f_*\gamma_*) \\ &\approx \left.\frac{\partial\kappa^{(n)}}{\partial f}\right|_{\substack{f = f_* \\ \gamma = \gamma_*}} \delta f\end{aligned}$$

$$+\left.\frac{\partial \kappa^{(n)}}{\partial \gamma}\right|_{\substack{f=f_* \\ \gamma=\gamma_*}} \delta\gamma, \qquad \text{(A.3)}$$

when the parameters f and γ vary on δf and $\delta\gamma$, respectively. If the arguments of the partial derivatives of the function $\kappa^{(n)}(f, \gamma)$ in respect to the variable f and γ at the point $f = f_*$, $\gamma = \gamma_*$ are not equal

$$\arg\left(\left.\frac{\partial \kappa^{(n)}}{\partial f}\right|_{\substack{f=f_* \\ \gamma=\gamma_*}}\right) \neq \arg\left(\left.\frac{\partial \kappa^{(n)}}{\partial \gamma}\right|_{\substack{f=f_* \\ \gamma=\gamma_*}}\right). \qquad \text{(A.4)}$$

and if the values f_* and γ_* are strictly inside the interval $[0,1]$ (and therefore the variations δf and $\delta\gamma$ are arbitrary), then by choosing these variations we can give arbitrary direction to the variation $\delta\kappa^{(n)}(f_*, \gamma_*)$ of the position of the point $\kappa^{(n)}(f_*, \gamma_*)$. Therefore this point cannot be the boundary point of the track of the corresponding arc. It means that the necessary condition for the point $\kappa(f_*, \gamma_*)$ to be on the boundary of the track of the arc is $\gamma = 0$, or $\gamma = 1$ (in these cases the bounds are drawn by the end points (2.6) and (2.7) of the arcs (2.1)) or

$$\left[\frac{\partial \kappa^{(n)}}{\partial f}\left(\frac{\partial \kappa^{(n)}}{\partial \gamma}\right)^*\right]'' = 0. \qquad \text{(A.5)}$$

Last condition means that mentioned partial derivatives have the same arguments (we recall that the star in the expression a^* denotes the complex conjugate to a). It is clear from the expression (2.1) that the whole problem degenerates if $f = 0$ or $f = 1$ and therefore we should not take these points into account.

The argumentation that we use here follows the work by Milton (1981) where the set of the values for the complex function depending on several real parameters were obtained.

The rest are straightforward calculations. First we define the internal points (if they exist) on each of the arcs (2.1) that may draw the bounds. Then we draw the lines defined by these points and add to this lines the arcs drawn by the end points (2.6) and (2.7) of the arcs (2.1). The outermost pair of all these lines gives us the desirable bounds, see Fig. 1.

Let us examine the condition (A.5) for all the arcs (2.1). One can check that

$$\frac{\partial \kappa^{(n)}}{\partial f} = \frac{(\kappa_1-\kappa_2)[\kappa_1+y^{(n)}(\gamma)][\kappa_2+y^{(n)}(\gamma)]}{[f\kappa_2+(1-f)\kappa_1+y^{(n)}(\gamma)]^2}, \qquad \text{(A.6)}$$

$$\frac{\partial \kappa^{(n)}}{\partial \gamma} = \frac{f(1-f)(\kappa_1-\kappa_2)^2}{[f\kappa_2+(1-f)\kappa_1+y^{(n)}(\gamma)]^2} \times \frac{\partial y^{(n)}(\gamma)}{\partial \gamma}. \qquad \text{(A.7)}$$

Substituting (A.6) and (A.7) into (A.5) we deduce that

$$\left[\frac{\partial \kappa^{(n)}}{\partial f}\left(\frac{\partial \kappa^{(n)}}{\partial \gamma}\right)^*\right]'' = H\left(\frac{[\kappa_1+y^{(n)}(\gamma)][\kappa_2+y^{(n)}(\gamma)]}{(\kappa_1-\kappa_2)[\partial y^{(n)}(\gamma)/\partial\gamma]}\right)'' = 0, \qquad \text{(A.8)}$$

where H is real and equals

$$H = \frac{f(1-f)|\kappa_1-\kappa_2|^4\,|\partial y^{(n)}(\gamma)/\partial\gamma|^2}{|f\kappa_2+(1-f)\kappa_1+y^{(1)}(\gamma)|^4}. \qquad \text{(A.9)}$$

It is clear that H is positive if $f \in [0,\ 1]$, $\gamma \in [0,\ 1]$ and equal to zero only in the trivial cases $f = 0$, $f = 1$, $\kappa_1 = \kappa_2$ or $\mu_1 = \mu_2$. Therefore condition (A.5) leads to the equation

$$\left(\frac{[\kappa_1+y^{(n)}(\gamma)][\kappa_2+y^{(n)}(\gamma)]}{(\kappa_1-\kappa_2)[\partial y^{(n)}(\gamma)/\partial\gamma]}\right)'' = 0. \qquad \text{(A.10)}$$

As we see, this equation depends only on the parameter γ and on the moduli of the original

materials and does not depend on the volume fraction f. The dependence on the parameter f disappears because it enters into Eq. (A.5) only in a nonnegative real coefficient H.

By substituting the definition (2.2) of the function $y^{(1)}(\gamma)$ into Eq. (A.10) for $n = 1$ we get

$$\Big(3\{\kappa_1+4[\gamma\mu_1+(1-\gamma)\mu_2]/3\} \times \{\kappa_2+4[\gamma\mu_1+(1-\gamma)\mu_2]/3\} \times [4(\kappa_1-\kappa_2)(\mu_1-\mu_2)]^{-1}\Big)'' = 0. \qquad \text{(A.11)}$$

The last equation can be treated as a quadratic equation $A_1\gamma^2 + B_1\gamma + C_1 = 0$ for the parameter γ where the coefficients A_1, B_1 and C_1 are defined by the equation (2.9). The solutions γ_* and γ_{**} of this equation are described by (2.8) and (2.9).

If γ_* (or γ_{**}) belongs to the interval $[0,1]$ it defines the internal point $\kappa^{(1)}(f,\ \gamma_*)$ (or $\kappa^{(1)}(f,\ \gamma_{**})$) on the arc $\kappa^{(1)}(f,\ \gamma)$ (f is fixed, $\gamma \in [0,1]$). The arcs $\kappa^{(1)}(f,\ \gamma_*)$, $f \in [0,1]$ or $\kappa^{(1)}(f,\ \gamma_{**})$, $f \in [0,1]$ which are drawn by either of these points may form the bound for the $\widehat{G}(\kappa)$ set. Note (comparing (1.5) and (2.1)) that each of them passes through the points κ_1 and κ_2 of the original materials. In addition the first arc passes through the point $-y^{(1)}(\gamma_*)$, i.e., it can be described as

$$\mathrm{Arc}(\kappa_1,\ \kappa_2,\ -y^{(1)}(\gamma_*))$$

and the second one passes through the point $-y^{(1)}(\gamma_{**})$, i.e., it can be described as

$$\mathrm{Arc}(\kappa_1,\ \kappa_2,\ -y^{(1)}(\gamma_{**})).$$

By substituting (2.3) into (A.10) for $n = 2$ we deduce after simple calculations

$$\Big(4[1/\kappa_1+3\gamma/(4\mu_1)+3(1-\gamma)/(4\mu_2)] \times [1/\kappa_2+3\gamma/(4\mu_1)+3(1-\gamma)/(4\mu_2)] \times [3(1/\kappa_1-1/\kappa_2) \times (1/\mu_1-1/\mu_2)]^{-1}\Big)'' = 0. \qquad \text{(A.12)}$$

As we see this equation is also independent of the volume fraction. Moreover, comparing (A.11) and (A.12) we can see that they coincide if we replace κ_1, κ_2, $4\mu_1/3$, and $4\mu_2/3$ in expression (A.11) by

$$1/\kappa_1,\ 1/\kappa_2,\ 3/(4\mu_1), \quad \text{and} \quad 3/(4\mu_2),$$

respectively. Therefore by changing the variables in formulas (2.9) and (2.8) we find that condition (A.12) is equivalent to the quadratic equation $A_2\gamma^2 + B_2\gamma + C_2 = 0$ where the coefficients A_2, B_2, and C_2 are defined by (2.11). The solutions $\widehat{\gamma}_*$ and $\widehat{\gamma}_{**}$ of this equation are defined by (2.10) and (2.11).

If $\widehat{\gamma}_*$ (or $\widehat{\gamma}_{**}$) belongs to the interval $[0,1]$ then the points $\kappa^{(2)}(f,\ \widehat{\gamma}_*)$ and $\kappa^{(2)}(f,\ \widehat{\gamma}_{**})$ draw the bounds of the region drawn by the arc $\kappa^{(2)}(f,\ \gamma)$, (f is fixed, $\gamma \in [0,1]$) when f varies from 0 to 1. Therefore these arcs $\kappa^{(2)}(f,\ \widehat{\gamma}_*)$, $f \in [0,1]$ or $\kappa^{(2)}(f,\ \widehat{\gamma}_{**})$, $f \in [0,1]$ may form the bounds for the $\widehat{G}(\kappa)$ set. Note (comparing (1.5) and (2.1)) that each of them passes through the points κ_1 and κ_2 of original materials. In addition the first arc passes through the point $-y^{(2)}(\widehat{\gamma}_*)$, i.e., it can be described as $\mathrm{Arc}(\kappa_1,\ \kappa_2,\ -y^{(2)}(\widehat{\gamma}_*))$, and the second one passes through the point $-y^{(2)}(\widehat{\gamma}_{**})$, i.e., it can be described as $\mathrm{Arc}(\kappa_1,\ \kappa_2,\ -y^{(1)}(\widehat{\gamma}_{**}))$.

One can also check that by substituting (2.4) into (A.10) we arrive at the equation

$$\{-\gamma + [(3\kappa_1/4+\mu_1)(\kappa_2+4\mu_2/3)] \times [(\kappa_1-\kappa_2)(\mu_2-\mu_1)]^{-1}\}'' = 0. \qquad \text{(A.13)}$$

Obviously the last expression does not depend on γ and has no solution. Therefore the only points on the arc (2.1), $n = 3$, that we should take into account when we construct the $\widehat{G}(\kappa)$ set, are the points $\gamma = 0$ and $\gamma = 1$. They correspond to the arcs (2.6) and (2.7). The same is true for the function $\kappa^{(4)}(f,\ \gamma)$, see (2.1) $n = 4$.